Electronic Supplementary Information (ESI)

Amorphous zeolite imidazole framework derived hierarchically porous, multi-catalytic active site bifunctional catalysts for zinc-air batteries

Supeng Ye, Yunxian Zhang, Fei Lin, Yingjian Huang, Xuelong Zhou, Qixing Wu and Fang Wang*

College of Chemistry and Environmental Engineering, Shenzhen University, Shenzhen 518000, Guangdong, China

*Corresponding author.

E-*mail address:* wangfsz@szu.edu.cn (Prof. F. Wang).

Keywords: Zinc-air batteries, Bifunctional catalysts, Amorphous ZIFs, CoFe alloy, Hierarchical pores

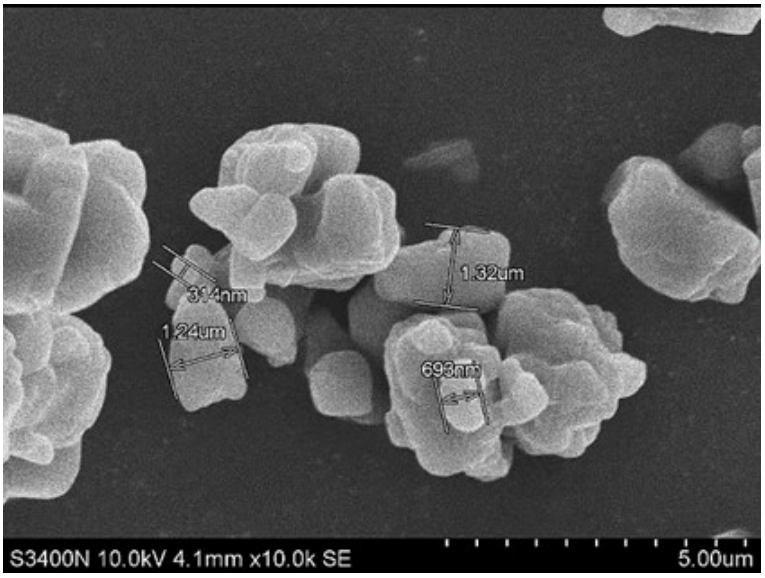

Fig. S1 SEM images of nanoscale NaCl.

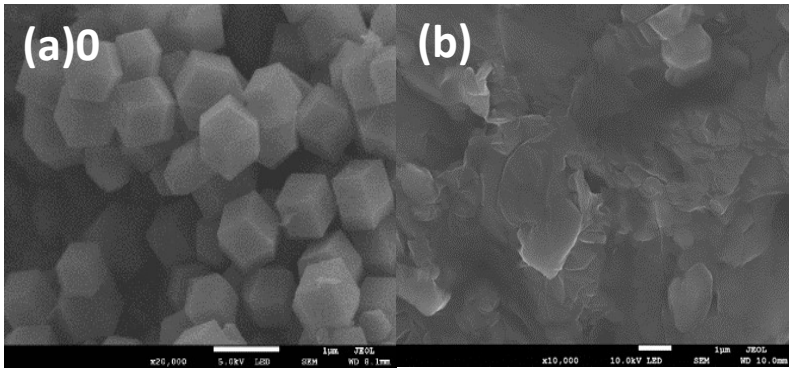

Fig. S2 SEM images of (a) ZIF-67 and (b)amorphous ZIF-67.

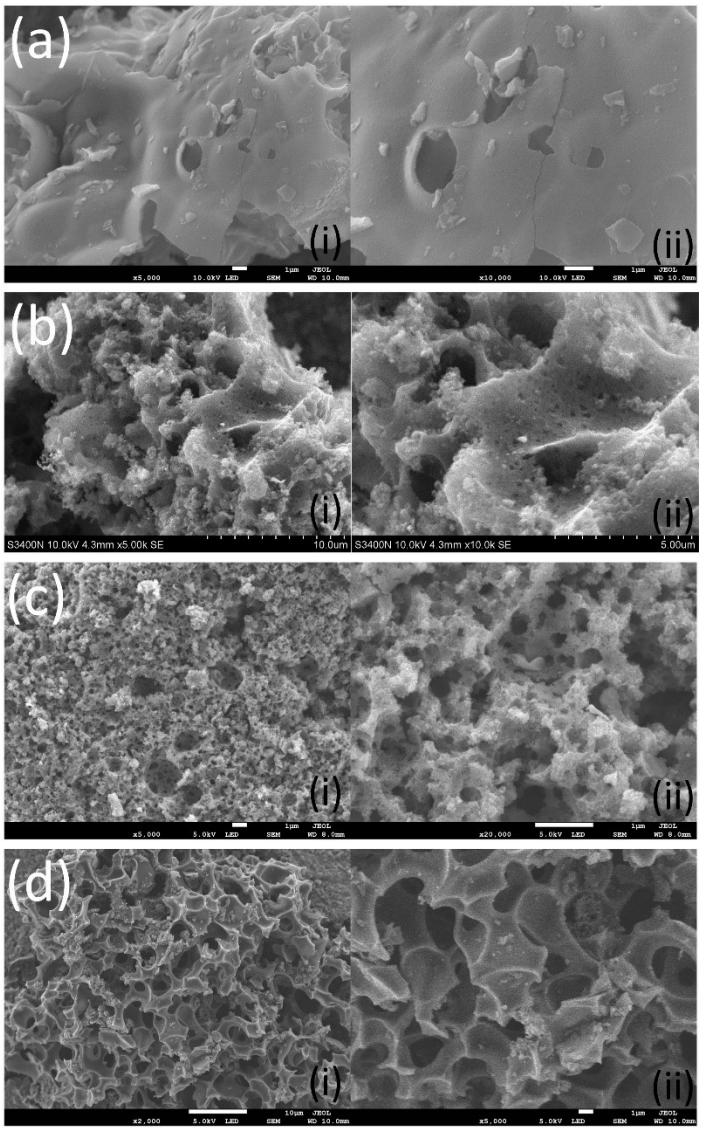

Fig. S3 FESEM images of HP/CoNC with different addition of NaCl templates: (a) 0 mmol, (b) 0.5 mmol, (c) 0.85 mmol and (d) 1.5 mmol.

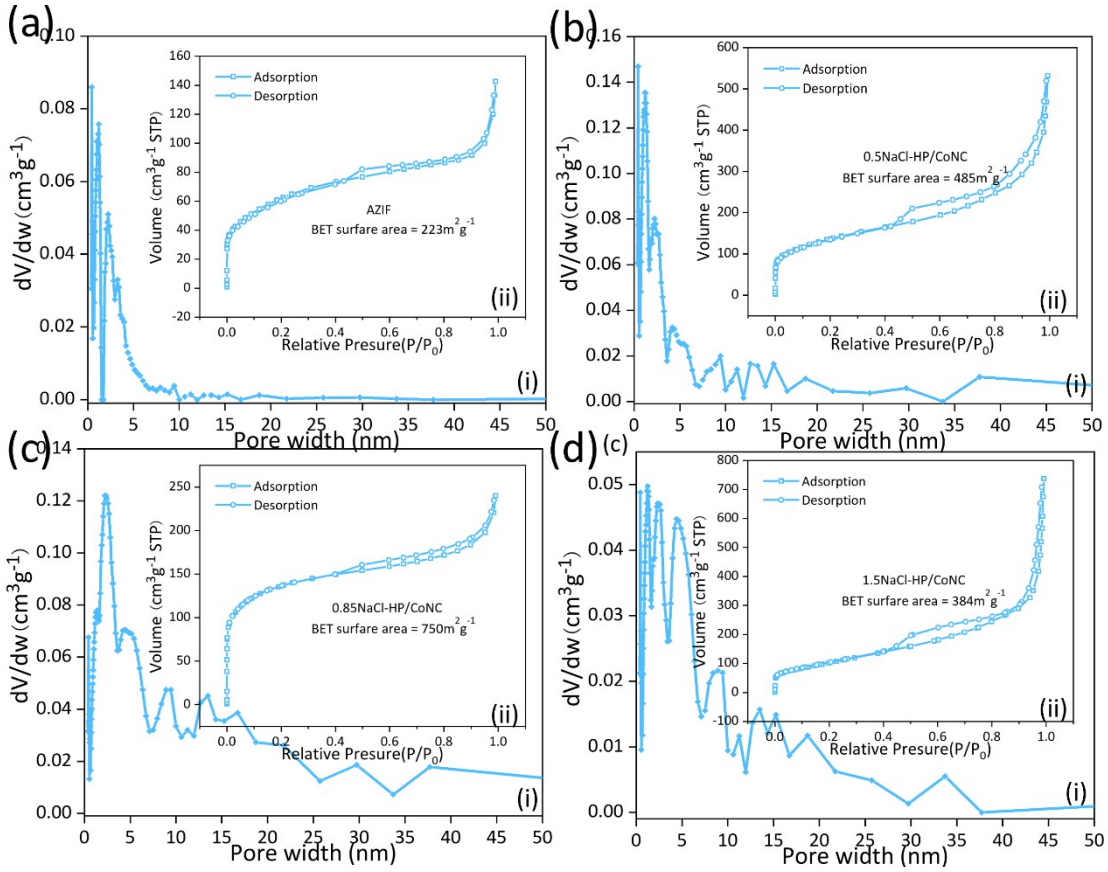

Fig. S4 N_2 adsorption and desorption curves (ii) and pore size distribution curves (i) of HP/CoNC with different addition of NaCl templates: (a) 0 mmol, (b) 0.5 mmol, (c) 0.85 mmol, (d) 1.5 mmol.

As shown in **Fig. S3 and S4**, the catalyst sample without the addition of NaCl is flat and smooth, showing inapparent porous structure, while the three groups of samples with the addition of NaCl templates appear more obvious porous structure. Among them, the catalyst using 0.85 mmol NaCl templates has evenly and densely distributed macropores and mesopores, which has the largest specific surface area. When 0.5 and 1.5 mmol NaCl was added, neither too little nor excessive templates are favorable for the formation of mesopores, thus 0.85 mmol NaCl was used in our research. So the addition of NaCl templates play a key role in the construction of hierarchical porous structure.

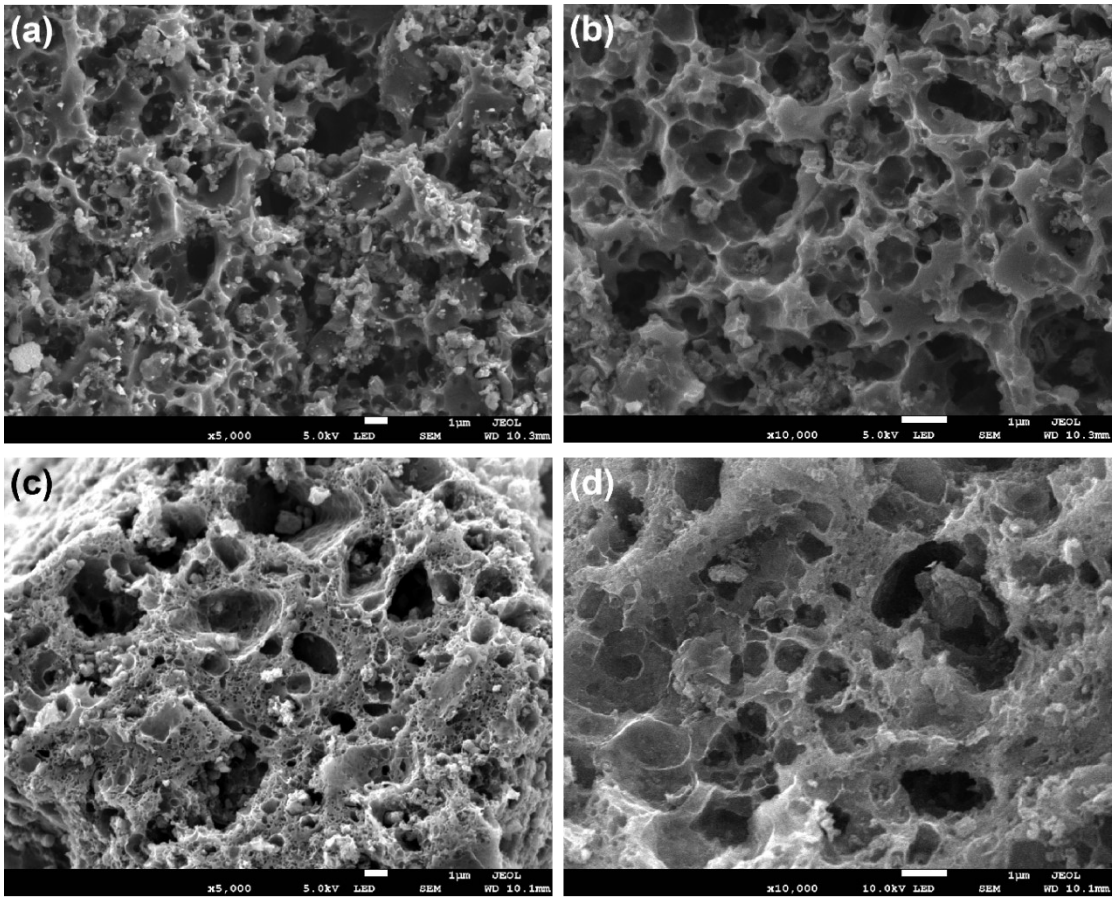

Fig. S5 SEM images of (a) HP/CoNC, (b) CoFe-1@HP/CoNC, (c) CoFe-2@HP/CoNC and (d) CoFe-3@HP/CoNC.

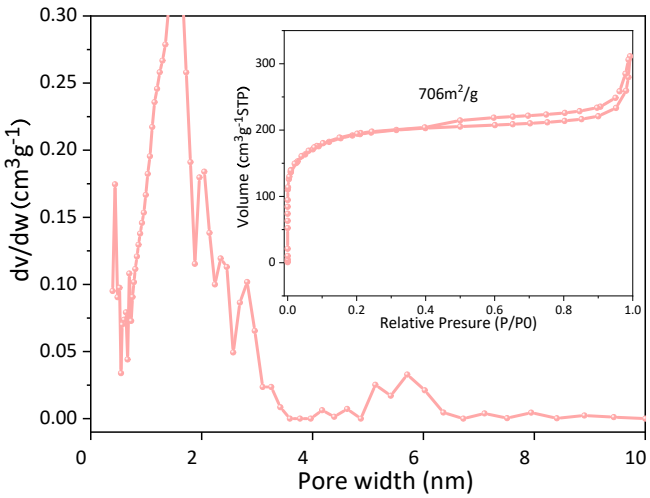

Fig. S6 N_2 adsorption/desorption isotherms and pore size distribution of CoFe-1@HP/CoNC.

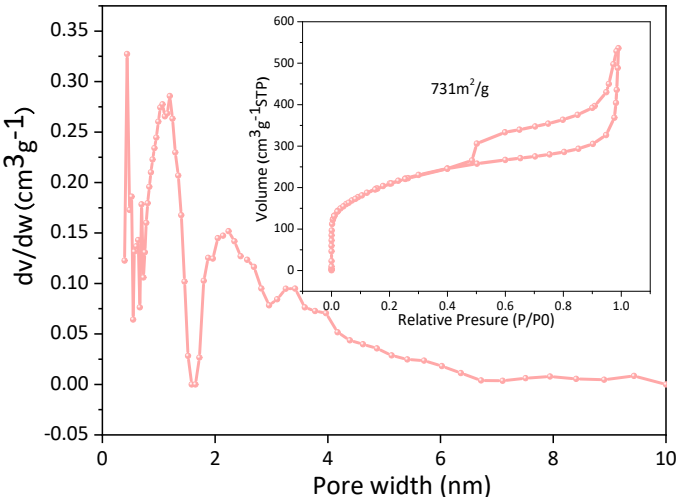

Fig. S7 N_2 adsorption/desorption isotherms and pore size distribution of CoFe-3@HP/CoNC.

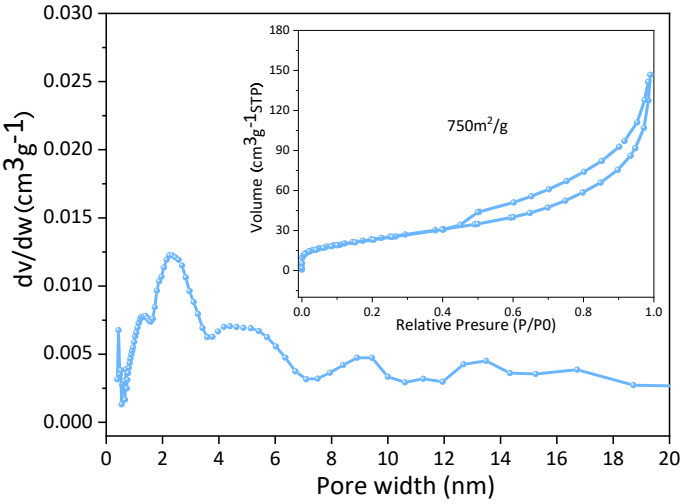

Fig. S8 N_2 adsorption/desorption isotherms and pore size distribution of HP/CoNC.

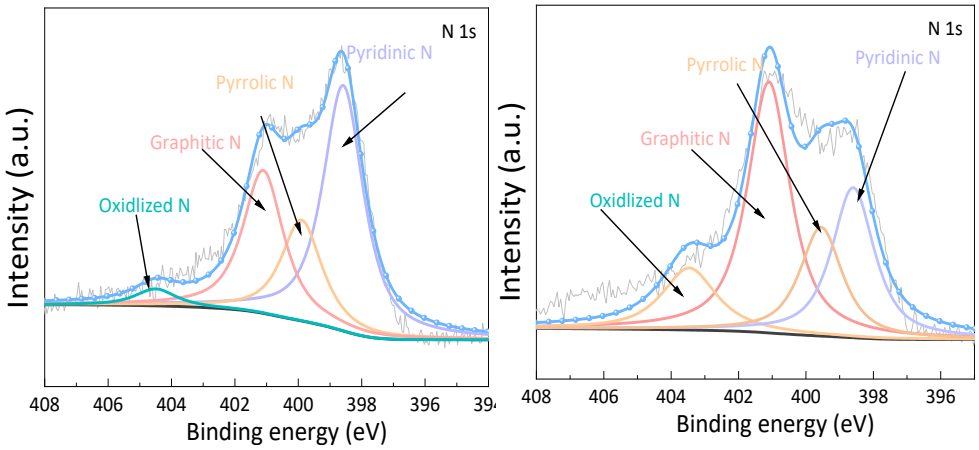

Fig. S9 N 1s high-resolution XPS spectrum of (a) CoFe-1@HP/CoNC, (b) CoFe-3@HP/CoNC.

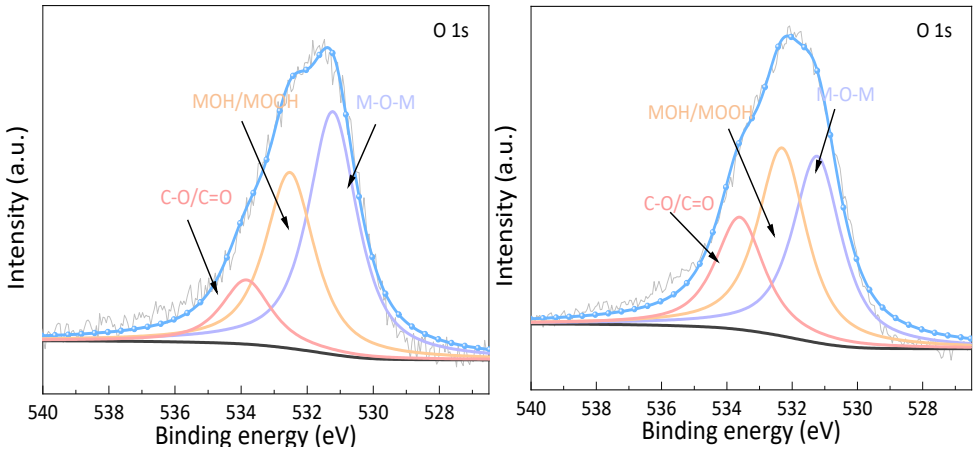

Fig. S10 O 1s high-resolution XPS spectrum of (a) CoFe-1@HP/CoNC, (b) CoFe-3@HP/CoNC.

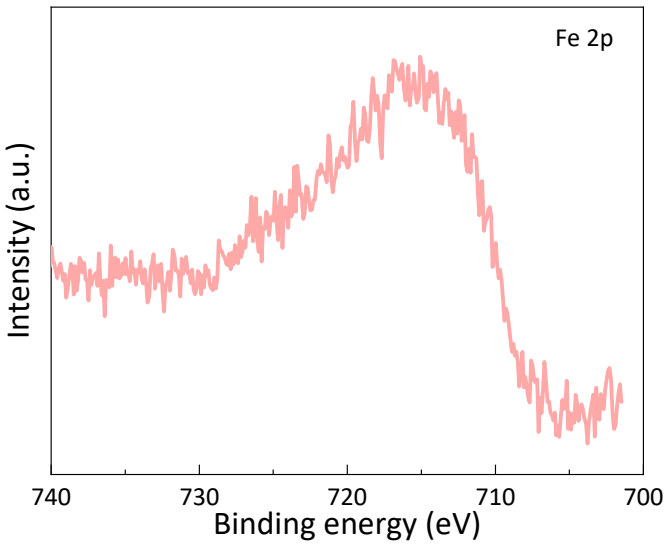

Fig. S11 High-resolution XPS spectrum of Fe 2p.

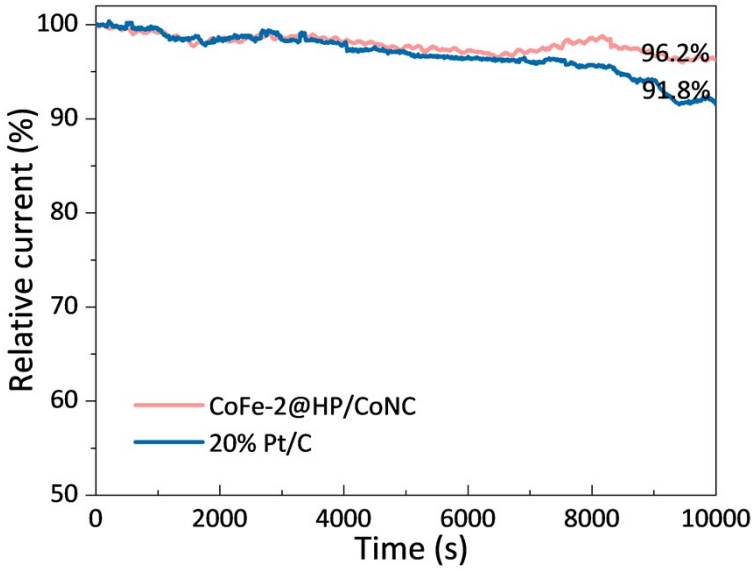

Fig. S12 Chronoamperometric responses of CoFe-2@HP/CoNC and Pt/C at 0.68V (vs. RHE) in O_2-saturated 0.1 M KOH.

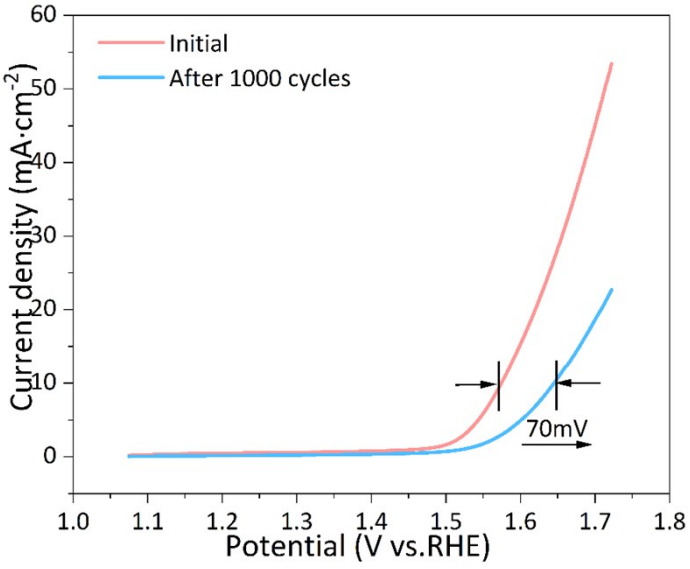

Fig. S13 Cyclic stability test of IrO_2 in 1 M KOH.

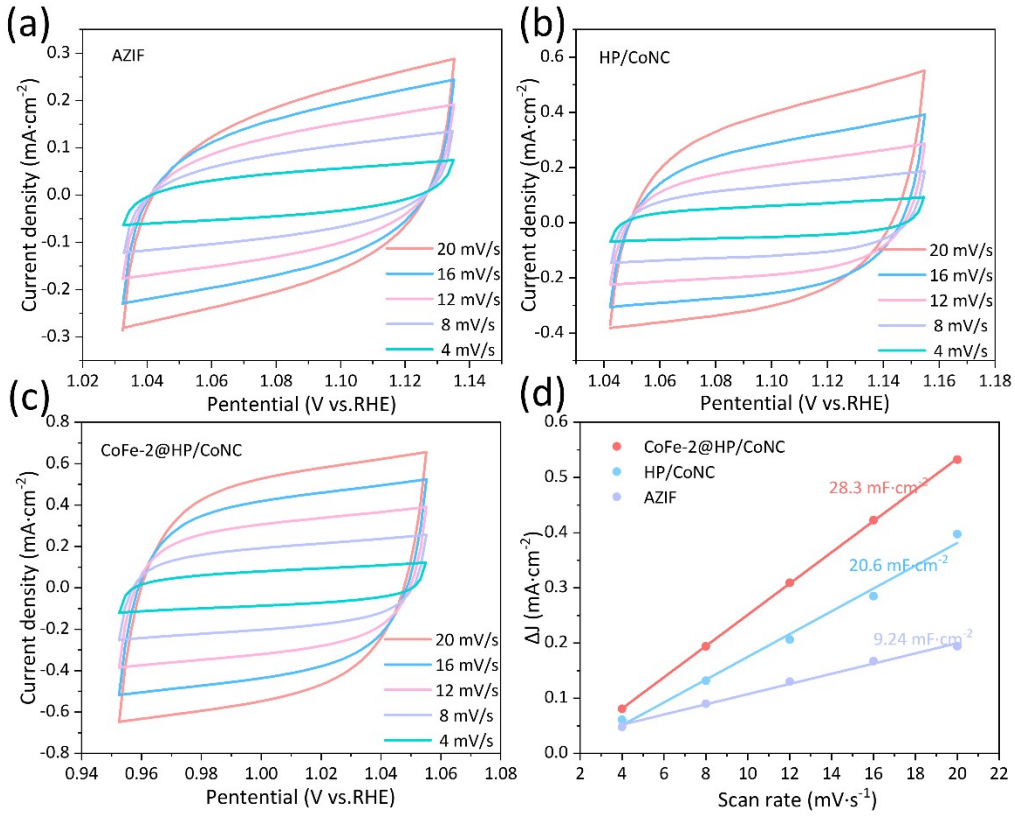

Fig. S14 CV curves of (a) AZIF, (b) HP/CoNC and (c) CoFe-2@HP/CoNC at different scanning speeds in the non-Faraday voltage range. (d) C_{dl} of CoFe-2@HP/CoNC , HP/CoNC and AZIF.

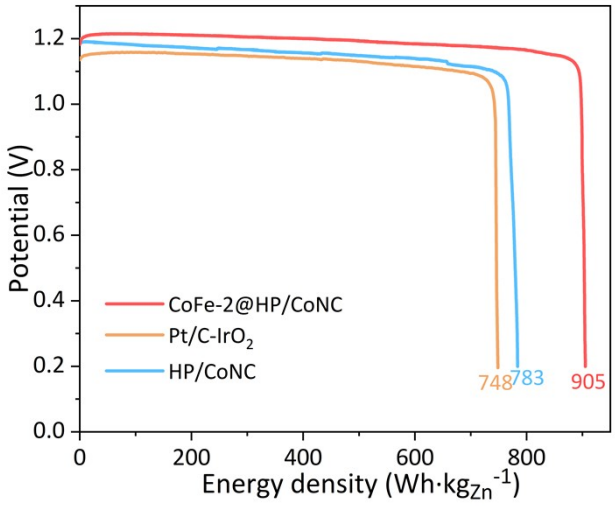

Fig. S15 Energy density of ZABs normalized to the weight of Zn.

Table S1 Atomic compositions of the prepared catalysts obtained from XPS spectra.

samples	C 1s (At. %)	N 1s (At. %)	O 1s (At. %)	Co 2p (At. %)	Fe 2p (At. %)
HP/CoNC	84.03	9.60	5.29	1.09	0
CoFe-1@ HP/CoNC	83.25	9.20	6.05	1.04	0.45
CoFe-2@ HP/CoNC	81.44	9.27	7.46	1.28	0.55
CoFe-3@ HP/CoNC	84.92	6.16	7.59	0.70	0.63

Table S2 A survey of zinc-air batteries assembled by different electrocatalysts.

Catalyst	Open-circuit Voltage (V)	Peak power density ($mW \cdot cm^{-2}$)	Specific capacity ($mAh \cdot g_{Zn}^{-1}$)	Stability-Current density ($mA \cdot cm^{-2}$)	References
CoFe-2@HP/CoNC	**1.512**	**221.3**	**760.7**	**450h-5 150h-10**	**This work**
Pt/C-IrO_2	**1.420**	**146.6**	**657.3**	**80h-5**	
$CuMo_2ON$@NG	1.438	176.3	736	330h-10	Nano Energy 2021; 85:105987.
FeNi-SAs@NC	1.54	260	950	100h-20	Energy Storage Materials 2021; 35:723-730
CoFe-LDH@CoFeNPs-N-CNTs	1.51	116	799	100h-10	Small 2021; 17(44):2103737
Co-SAs/SNPs@NC	1.493	223.5	742	720h-5	Advanced Functional Materials 2021; 31(45):2104735
Fe/Ni(1:3)-NG	1.50	164.1	824.3	120h-5	Carbon 2021; 185:526-535.
CoFe/NSC	1.45	162.74	776	150h-5	Journal of Energy Chemistry 2021; 56:64-71
ZOMC	1.49	221.1	795.3	150h-5	Advanced Materials 2020; 32(28):2002170